Direct Observation of Microscopic Solvation at the Surface of Clusters by Ultrafast Photoelectron Imaging†

Lionel Poisson,‡ Eric Gloaguen,‡ Jean-Michel Mestdagh,‡ Benoît Soep,*,‡ Alejandro Gonzalez,§ and Majed Chergui§

Laboratoire Francis Perrin (CNRS-URA-2453), DSM/IRAMIS/Service des Photons, Atomes et Molécules, C.E.A. Saclay, F-91191 Gif-sur-Yvette Cedex, France, and Ecole Polytechnique Fédérale de Lausanne, Laboratoire de Spectroscopie Ultrarapide, ISIC, Faculté des Sciences de Base, BSP CH-1015 Lausanne-Dorigny, Switzerland

Received: November 28, 2007; Revised Manuscript Received: March 17, 2008

We report on microscopic observation of solvation by argon atoms of excited states of an ethylenic-like molecule, TDMAE (tetrakis dimethylaminoethylene). Two experimental methods were used: gas phase dynamics for the observation of the evolution through excited states, matrix isolation spectroscopy for characterization of the initial states. Excited state dynamics was recorded after the molecule had been deposited on the surface of a large argon cluster ($n \approx 100$) by pick-up. The deposited cluster was characterized by mass spectrometry and by its shifted photoelectron spectrum. The time evolution of the system was visualized by femtosecond pump/probe velocity map imaging of photoelectrons. The time evolution of deposited TDMAE excited at 266 nm can be modeled via a modified three state model, as in the free molecule. The initially excited state is of valence character, and a Rydberg state mediates the passage to a zwitterionic configuration. The specific solvation of Rydberg states by the surface of the cluster was directly observed and is discussed. It represents the striking outcome of the present work. It is inferred that differently from the gas phase, solvated Rydberg states resulting from state mixing within a $R_{n/\lambda}$ complex in the presence of the argon surface are reached. Solvation of these Rydberg states should be effective through interaction of the ion core of the excited molecules with the cluster.

Introduction

The electronic excitation of polyatomic molecules is generally followed by relaxation of the electronic energy to the ground state or to metastable low lying states such as triplet states in hydrocarbons. This determines their photochemical and photobiological properties where the reactivity of the originally excited state is low due to efficient competition with fast relaxation processes. This is especially true for highly excited states. The relaxation is driven by nonadiabatic processes, where the great number of molecular modes of polyatomic molecules can couple the electronic configurations of the initial and final states.

The theory of these processes has been well-established for isolated molecules.[1] Two major mechanisms are at play involving both nonadiabatic processes. In the first, the relaxation occurs as a tunnelling process between the two relevant states through many oscillations of the vibrations, or it can proceed directly via the intersection of excited surfaces.[2] In the first process, each vibration has a small coupling efficiency, and the global efficiency is derived from the number of coupled modes. This compares more with a dissipative, statistical mechanism. In the second mechanism, a wavepacket is prepared on the initially excited surface and descends rapidly through the seam of crossing to the lower surface, driven by surface gradients.

Since, in general, relaxation is observed in condensed phases, it is essential to conduct the relevant experiments in the presence of a perturbing medium. Experiments have been conducted so far either in the isolated limit case or in the condensed phase liquid or matrix or crystal. The systematic investigation of the effects of the medium at experimental or theoretical levels is not an overstudied theme, by far, although several authors have sought to address it at a microscopic level. The effects of the medium can be ascribed to many factors: the increased density of levels in a condensed medium and the level broadening by collisions. There, the medium can be considered as passive and only provides a continuum to match the energy of the initial and final states.[3,4] On the other hand, the potential energy surfaces can be solvated differently by the medium, or the coupling between the configurations can be strongly affected by it. This active effect of the medium should be specifically at play when one of the electronic configurations is ionic or Rydberg and is thus strongly affected by the medium.

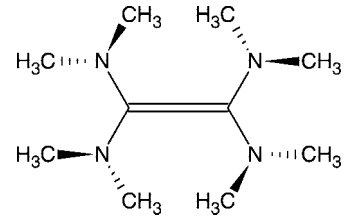

Figure 1. TDMAE molecule.

We shall address such a problem here, the coupling of excited configurations in a molecule possessing charge transfer intermediates, zwitterionic states, and Rydberg states, with a microscopic solvating medium. This molecule is tetrakis dimethylaminoethylene (TDMAE), shown in Figure 1. We per-

* Corresponding author. E-mail: Benoit.Soep@cea.fr.
† Part of the "Stephen R. Leone Festschrift".
‡ Laboratoire Francis Perrin.
§ Ecole Polytechnique Fédérale de Lausanne.

10.1021/jp711259m CCC: $40.75
Published on Web 06/24/2008

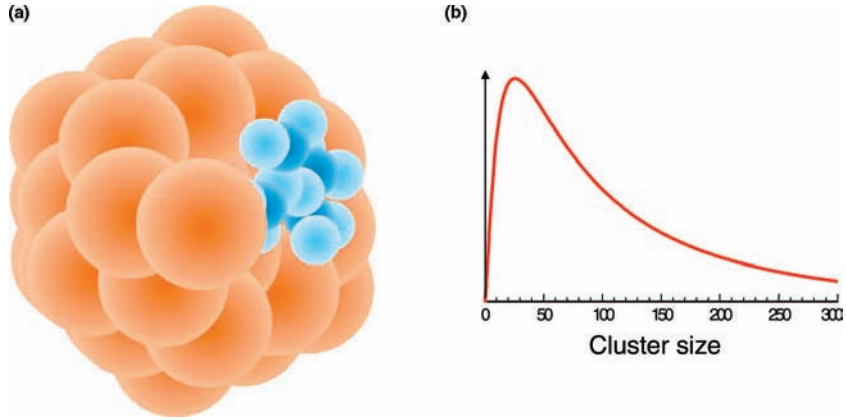

Figure 2. (a) Schematic scaled representation of the TDMAE molecule deposited on an argon cluster after pick-up. The TDMAE molecule almost matches a surface substitution site of argon. The average size is in general estimated to be ~100−200 atoms. For convenience, a 50 atom cluster is pictured here. (b) Log normal distribution of argon clusters in supersonic expansion (av size $n = 100$, fwhm 100).

formed two types of measurements on TDMAE solvated by argon: steady state measurements in an argon matrix environment and time-resolved experiments on TDMAE−argon surface clusters (Figure 2) to monitor dynamic solvation in this microenvironment.

TDMAE was chosen because of the generic properties of ethylene-like molecules caused by their electronic state configurations. Indeed, ethylene has long been recognized as displaying a conical intersection between the valence $\pi\pi^*$ state (V of $C^{\bullet}-C^{\bullet}$ biradical type) and a zwitterionic state (Z, $C^{+}-C^{-}$). The latter intersects with the ground state (N) and causes dissipation of electronic energy.[5–9] The decay of excited valence states in ethylene-like molecules is very fast [10–15] due to this excited state scheme combined with a large change in geometries between the V and Z configurations. This sets the best conditions for the intersection of surfaces on which the wavepacket movements can be very fast (20 fs), as for ethylene for which the relevant torsional movements have very little inertia.[10,11]

Owing to its very low ionization potential (5.4 eV[16]), TDMAE displays increased interactions between the V and Z configurations. The electronic relaxation from an initially excited V $\pi\pi^*$ state leads to a Z state, but this decay is mediated by a diffuse, Rydberg state[5,7,17–19] (R). This behavior was determined through time-resolved photoelectron spectroscopy of supersonically cooled TDMAE.[20] Also, we wished to keep the potentialities of techniques such as photoelectron spectroscopy to investigate the flow of energy over electronic states in the presence of a perturbing medium. These techniques are generally difficult to apply in clusters owing to size distributions that average the properties, especially in small clusters.[21] Thus, we used the largest clusters to overcome this difficulty. We also emphasize that the experimental methodology employed here (pick-up) favors the formation of surface deposited TDMAE and is far less sensitive to size effects than interior clusters. To date, very scanty results have been reported on photoelectron spectroscopy in the presence of a medium.[22,23] The solvation of halide anions away from the surface of water or clusters was investigated by photoelectron spectroscopy,[24,25] and solvated electrons were characterized at the surface of clusters by photoelectron imaging.[26]

The results presented in this paper demonstrate that photoelectron detection of deposited molecules can be achieved at the surface of argon clusters. The effect of the cluster is described by comparing the photoelectron spectra of free TDMAE with those of TDMAE deposited at the surface of the argon cluster. Time-dependent solvation of a Rydberg intermediate state of the molecule in the presence of argon is highlighted. Solvation by an infinite medium of argon also was performed by embedding TDMAE in argon crystals where, due to its size, the molecule was embedded in a disubstitutional site. The solvation shifts provided by matrix isolation spectroscopy were used to identify the nature of the electronic states. On one hand, valence states and ionic states are, respectively, weakly and strongly red shifted in going from the gas phase to matrices.[27,28] On the other hand, Rydberg states are characterized by strong blue shifts, which increase with the decreasing size of the matrix cage.[29] Therefore, we compare the UV spectra of TDMAE in the gas phase, and in rare gas matrices, to assign the valence and Rydberg transitions of the molecule. Such an observation of the solvation of excited states of a molecule at a very microscopic level is a key element in the photochemistry of highly polarized compounds.

Experimental Conditions

Matrix Isolation Spectra. For matrix isolation spectroscopy, the vapor of TDMAE at room temperature (pressure of 0.3 mbar) was premixed with the rare gas at ratios of 1:2000−1:5000, and the mixture was condensed onto an LiF window cooled by a liquid helium flow in an ultrahigh vacuum chamber. Optically transparent samples were grown at 5 K for Ne, 20 K for Ar, and 25 K for Kr. An Acton Research UV−vis monochromator equipped with a 600 lines/mm grating, blazed at 150 nm, and a stabilized D_2 lamp were used for absorption measurements. Spectra were recorded with a UV-enhanced CCD camera. For the measurements of gaseous TDMAE, we used a 10 cm cell with quartz windows for transmission, and the spectra were recorded with a Shimadzu spectrophotometer.

Time-Resolved Cluster Experiments. Argon clusters were generated by a pulsed supersonic expansion of high pressure argon gas (up to 12 bar) through a 100 μm nozzle. Average cluster sizes were evaluated using the empirical relations derived by Hagena[30] and Buck and Krohne[31] for continuous expansions. We applied a correction factor of 2, taking into account the pulsed expansion. This resulted in average argon cluster sizes of ca. 100. The distribution in sizes is represented in general by a log-normal function as shown in Figure 2b. As we shall see later in this paper, the accurate determination of the cluster size is not an important issue for the present work.

The TDMAE gas (0.2 mbar) was introduced in the expansion chamber by a tube that was shaped to a rectangle (2 mm × 1 mm) and placed close to the nozzle. The molecules were

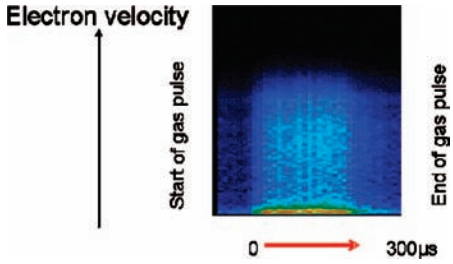

Figure 3. 266/400 nm pump/probe photoelectron detection of TDMAE deposited on argon clusters. Horizontal: delay between the pulse valve and the ionization lasers. Vertical: kinetic energy release of the electrons. The intensities are in false colors (white is most intense).

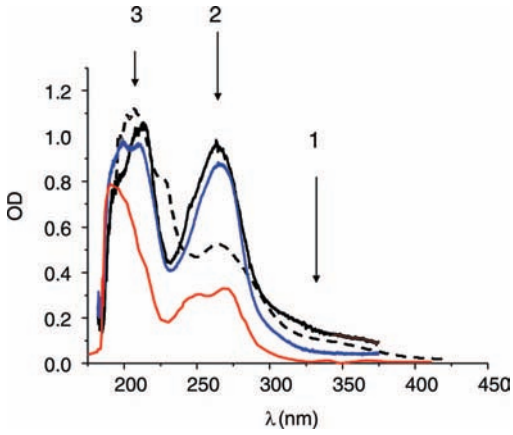

Figure 4. Comparison of gas phase, room temperature absorption of TDMAE (dashed line) and TDMAE in a Krypton matrix (black), an argon matrix (blue), and a neon matrix (red). The three main bands are labeled as discussed in the text.

captured by clusters of large dimensions (20 Å in diameter) and subsequently cooled by evaporation of argon atoms from the cluster surface. If one evaluates the energy content of the molecule as ~6000 cm^{-1}, the cooling will evaporate 15 argon atoms. This considers that each argon atom has been evaporated from the surface and interacted with 8 atoms with 100 cm^{-1} energy in the Ar−Ar bond. The probability of picking up a molecule is a fraction of unity in our experimental conditions; the number density of TDMAE is 1/10 of that of the clusters. Hence, the fraction of clusters carrying more than one TDMAE is negligible. The clusters are illustrated in Figure 2a.

The diffusion of TDMAE in the experiment chamber was suppressed by the use of cryo-cooling, which brings down the background electron signal to very low values, 1/100 of the total count number of the deposited TDMAE signal. This can easily be monitored by observing the background signal recorded immediately before the opening of the pulse valve (see following discussion and Figure 3).

Photoelectron imaging has been the preferred, most sensitive diagnostic for the time evolution of deposited clusters, despite the absence of mass resolution. In addition to the characterization of the electronic state provided by photoelectrons, the sensitivity of electron detection is greater since all electrons are detected. This is not the case for the larger clusters ions with a mass >2000 (50 Ar), which have a much poorer detectivity on microchannel plates and also cannot be correctly focused on the detector.

The angle averaged photoelectron spectrum is represented as a function of the laser−valve time delay in Figure 3. It was seen that before the opening of the valve, there remained a negligible signal owing to the efficient cryo-cooling of the experiment chamber previously mentioned. If in turn we monitored the ions ranging from $TDMAE^+$ to TDMAE-Ar_n^+, the ratio would be far less favorable.

It easily was verified that the photoelectron signal pertains to large Ar_n clusters with TDMAE. If the total ion signal is recorded as a function of the valve opening and compared with the equivalent electron signal, very few ions are detected during the gas pulse. This shows that the observed electrons relate to high mass ion deposited clusters.

Time Evolution. Femtosecond pump/probe experiments were performed at the LUCA facility in Saclay on the systems under study. The clusters were excited at 266 nm with a typical energy of 30 μJ in a 0.5 mm diameter spot. The evolution was probed by 400 or 800 nm pulses with a 100 fs cross-correlation width fwhm. The setup is described in ref 20 and was used essentially to detect photoelectrons by velocity map imaging.

Data Analysis of Time-Resolved Photoelectron Spectra. Photoelectron spectra were recorded for TDMAE deposited on Ar_n clusters, averaged over a range of cluster sizes as previously mentioned. The set of raw images was transformed by the Abel inversion using the pBasex[32] procedure. Thus, the angular distribution created by the laser absorption has the following form, expanded in terms of Legendre polynomials:

$$I(\theta) = 1/4\pi(P_0 + P_2(\cos\theta)) \quad (1)$$

As a reference, $\beta \cong 0.8$ for the Z state of gas phase TDMAE. The pBasex program allows for the extraction of angular dependence (i.e., Legendre polynomial coefficients of orders of 0 and 2, respectively, P_0 and P_2) in the form

$$I(E, t, \theta) = \alpha(E, t)(P_0 + \beta(E, t)P_2(\cos\theta)) \quad (2)$$

where E is the electron energy, t is the pump/probe delay, and θ is the angle between the polarization of the ionization laser and the direction of the electron recoil. The pBasex program yields $\alpha(E,t)$ (termed the P_0 component or isotropic component) and $\alpha(E,t)\beta(E,t)$ (the P_2 component or anisotropic component). The P_0 isotropic term relates to the intensity of the photoelectron emission at a given energy and time, while the anisotropic term relates to the degree of alignment of the electrons with the ionizing field.

Results

The measurements described here are aimed at interpreting the electronic relaxation of an excited molecule in the presence of a perturbing medium by matrix isolation and femtosecond photoelectron spectroscopies.

Matrix Isolation Spectroscopy. UV absorption spectra of TDMAE were recorded in the gas phase and several rare gas matrices. Figure 4 compares the absorption spectra of TDMAE in the gas (dotted line) and in Ne, Ar, and Kr matrices. The gas phase spectrum exhibits three features, a broad shoulder at ~340 nm, a well-defined band at ~270 nm, and a band at ~220 nm, which extends further to the blue region (these bands are labeled 1−3 in the following discussion). This spectrum resembles the previously measured one by Nakato et al.,[16] which extends down to 170 nm, and clearly shows the three bands riding on a continuum absorption background, which they attributed to $\pi-\pi^*$ valence transitions. However, in our case, the background seems less prominent or even absent, which suggests that it may be due to impurities in their spectra. The three bands were attributed to Rydberg transitions, likely $3ns \leftarrow N$[16]. Because of their extended orbitals, Rydberg states are sensitive to external perturber effects that have long been used as a means to distinguish these states from valence or ionic states. In general,

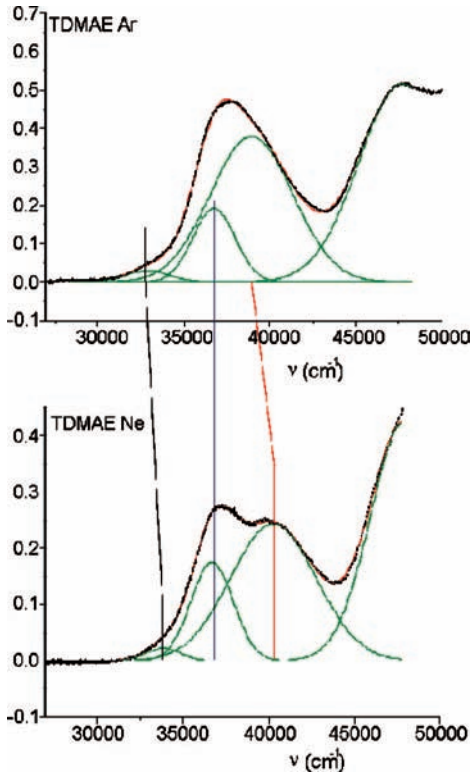

Figure 5. Matrix isolation absorption spectra of TDMAE deposited in argon (top) and neon (bottom). The experimental spectra are in black, and the simulations are the sum of four Gaussian components (three Rydbergs and one valence). The individual Gaussian components are shown in green and are found to be either insensitive to the nature of the matrix (blue vertical line corresponding to the V transition with a maximum at 271 nm in the matrix) or blue shifted in neon presumably due to the closer packing in this medium.

as a function of perturber density, bands belonging to transitions from the ground valence state to the Rydberg states show significant broadening, accompanied at high densities by blue shifts with respect to the transitions in the isolated molecule.[33] Isolation in a solid rare gas matrix represents a case of extreme density, manifested by the largest blue shifts and broadening.[29] Here, the matrix data show a number of features, some identical to the gas phase spectrum, others not: (a) band 1 (shoulder) at ~340 nm in the gas phase spectrum is very weakly distinguished in Ne matrices, but it becomes gradually more conspicuous in Ar and Kr matrices, although less clear-cut than in the gas phase. In the latter two matrices, it appears clearly blue shifted with respect to the gas phase. (b) The band in the gas phase at 265 nm turns out to consist of more than one component in the matrix spectra, as can clearly be seen in Ne matrices, where it is replaced by a doublet band, and in the slight asymmetry of the band in Ar and Kr matrices. This is more clearly seen in Figure 5, where the bands are fitted by a set of Gaussian line shapes. The low energy component does not show significant shifts from Ne to Ar matrices, as is known for valence bands, but the high energy component shifts to higher energies, as does band 1, which points to their Rydberg character.[29] (c) The third, high energy band, whose position is ill-defined, seems blue shifted in matrices with respect to the gas phase. In summary, the matrix data confirm the previous assignment by Nakato et al.,[16] for all three bands having a Rydberg character, but we see that band 2 in the matrix consists of two components in which one has valence character.

Time-Resolved Photoelectron Spectra. In a resonant two photon ionization of a molecule, the emitted electron contains very useful information on the intermediate excited state: the electron kinetic energy is correlated to the vibrational energy content of this state, and the orientation of the electron velocity vector with respect to the ionization field is sensitive to the electronic symmetry of the excited state.[12,20] The most sensitive method to follow the time evolution of a nonstationary electronic state is the time-resolved imaging device described previously. Several experiments have considered the energy shift of photoelectron spectra on clusters.[21,22] Aniline, for example, deposited on large helium clusters essentially displays the same spectrum but is broadened by phonons. Polarization effects of the ejected electrons and localization of the electron source at the interior or the surface of the cluster have not yet been discussed, to our knowledge. Cluster effects on the polarization of photodetached electrons from anion clusters have been observed,[34] and the depolarization was assigned to momentum transfer between the electron and the solvent molecules within the cluster.

The following measurements concern deposited TDMAE on argon clusters excited at 266 nm and ionized at 400 nm. First, the isotropic component P_0 informs us about the energy of the excited state. In Figure 6a, the time dependence of the isotropic component of the electron kinetic energy distribution, extracted from the images, is plotted as a function of time: $\alpha(E,t)$ versus pump/probe delay. At the longest delay times, the spectrum is composed of a peak at 0.9 eV superimposed on a continuum-like featureless band at lower energies. Just after the autocorrelation of the pump and probe lasers, the spectrum is only a broad, unsymmetrical feature with a maximum at ≈1.4 eV. Throughout the evolution, this broad structure transforms into a peak in 1500 fs. These features are exemplified in Figure 6b by cuts recorded at 0 fs (autocorrelation maximum of the pump and probe lasers) and 3200 fs, at the end of the evolution. It is also apparent in Figure 6a that a modulation of the spectrum is visible with a period of 500 fs; these oscillations are best seen close to zero energy and vanish after 2500 fs delays. Their intensity maxima are signaled by white bars in Figure 6a.

The same experiments were performed with a 800 nm probe, which had sufficient energy to ionize the V state by one photon in the bare molecule. Owing to solvation on the cluster, the energy of the electrons close to zero for the one photon ionization at 800 nm of the V state in the free molecule, was upshifted by 0.34 eV in the cluster. This allows for observation of the 250 fs temporal evolution of the V state. In addition, two 800 nm photons have the same effect as 400 nm in the free molecule. Indeed, we observed here that two 800 nm photons yielded the same evolution characteristics as in Figure 6. We thus extended the observation to very long delay times; this shows that the energy of electrons from the Z state slightly decreases by 0.05 eV over time (20 ps) as appears in Figure 11.

Anisotropy in Angular Distribution Photoelectrons. The second information that can be extracted from the images is the angular distribution of the electrons with respect to the ionization laser. This distribution characterizes the nature of the outgoing wave of the ejected electron and by correspondence, the excited electronic state. Here, we were interested not by this electronic state, already examined previously,[20] but by its interaction with the argon medium of the cluster as revealed by the polarized electron emission from the deposited molecule.

The full electron spectrum of deposited TDMAE between 0 and 1 eV does not originate from a single ionization mechanism, as suggested by its shape: some bands are superimposed on a continuum as appears in the time integrated spectrum of Figure

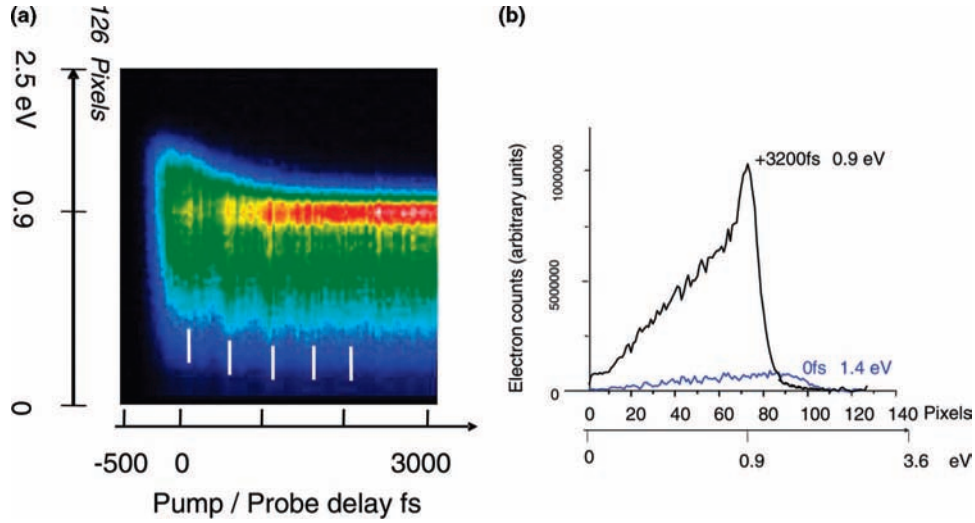

Figure 6. (a) Isotropic P_0 term in the time-resolved photoelectron spectrum of deposited TDMAE Ar_n (note that the vertical scale is nonlinear in energy, also indicated). The white vertical lines indicate maxima in intensity characteristics of wavepacket oscillations. (b) Cuts of the photoelectron spectrum at $t = 0$ and $t = 3200$ fs (horizontal scale nonlinear in energy, indicated as in panel a).

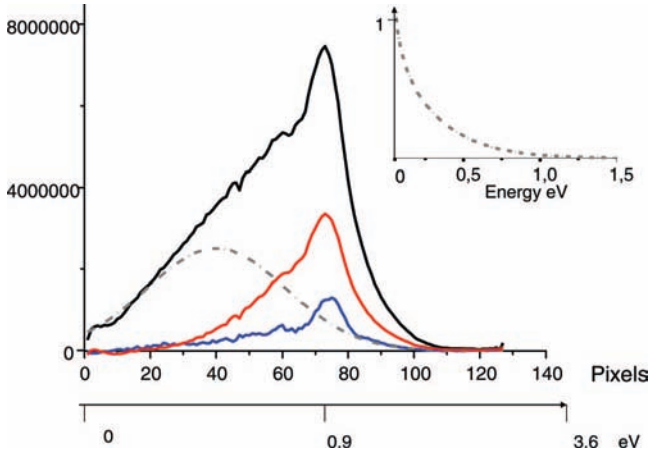

Figure 7. Time averaged photoelectron spectrum of deposited TDMAE as a function of the camera pixel number (i.e., in electron velocity space). The nonlinear energy scale is also indicated. Black: P_0 component, $\langle\alpha(E,t)\rangle_t$. Blue: P_2 component, $\langle\alpha(E,t)\cdot\beta\rangle_t$. Dashed−dotted: Gaussian function centered at pixel 40, 2 500 000 $\exp(-(\{x - 40\}/30)^2)$. Red: P_0 component was substracted with the Gaussian function. This corrected curve compares well with the blue curve representing the P_2 component of the spectrum (blue); see text. Inset: energy distribution corresponding to the Gaussian function.

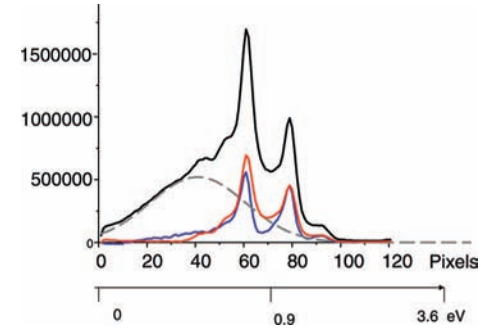

Figure 8. Time averaged photoelectron spectrum of free TDMAE as a function of the camera pixel number (i.e., in electron velocity space). Black: P_0 component, $\langle\alpha(E,t)\rangle_t$. Blue: P_2 component, $\langle\alpha(E,t)\cdot\beta\rangle_t$. Dashed−dotted: Gaussian function centered at pixel 40, 2 500 000 $\exp(-(\{x - 40\}/30)^2)$as in Figure 7. Red: P_0 component was substracted with the Gaussian function. This corrected curve compares well with the blue curve representing the P_2 component of the spectrum (blue); see text.

7. This Figure 7 displays the time integrated spectrum of the P_0 component derived from Figure 6, summed over all times. The same can be repeated for the P_2 component in Figure 7. We observed that the P_0 and P_2 time integrated spectra differ in shape, the latter one retaining only bands and almost no continuum. We thus assumed that the difference allowed us to distinguish between two different emission processes for the electrons I_I and I_{II} (discussed later in the text). Process 1: $I_I(E,t,\theta) = \alpha_1(E,t)P_0$ with no anisotropy. Process 2: $I_{II}(E,t,\theta) = \alpha_2(E,t)(P_0 + \beta_2(E,t)P_2(\cos\theta))$, with a second order P_2 (Legendre polynomial) angular dependence for the electron anisotropy, where the observed distribution is the sum $I(E,t,\theta) = I_I(E,t,\theta) + I_{II}(E,t,\theta)$.

The P_0 component has contributions from I_I and I_{II}, while the P_2 component relates only to I_{II}. Hence, the angular dependence of the time-resolved electron spectra was analyzed via the previously mentioned analysis of the electron angular distribution, to extract the sole I_{II} component.

This procedure was exemplified by the analysis of previous results on free TDMAE, where three bands appear in the photoelectron spectra and are also superimposed on a continuum at low electron energies. The time integrated P_0 spectral component of the electron images is represented together with the P_2 component, shown in Figure 8. We see that they differ in much the same way as before, and the P_2 spectrum is simpler with only well-defined bands, while the P_0 spectrum contains the same bands on a continuum. The two curves P_0 and P_2 can be made to resemble, by subtraction of a Gaussian function, I_I, centered at 40 pixels (0.28 eV) to the P_0 spectrum as seen in Figure 8. This yields a corrected isotropic spectrum, i.e., $\langle\alpha_2(E,t)\rangle_t$. The value of β_2 follows from the ratio of the P_2 component to this latter spectrum. The relative intensity of these two spectra, P_2 components/corrected P_0, yields $\beta = 0.8$ for the band centered at pixel 60 (0.68 eV), assigned to the Z state in ref 8.

It can thus be concluded that most of the background is due to an isotropic component in the angular distribution of the electron emission in the free molecule, pertaining to a different electron emission process. We applied this procedure in Figure 7, for TDMAE deposited on Ar_n, and also the anisotropic and corrected isotropic electron spectra match as in Figure 8.

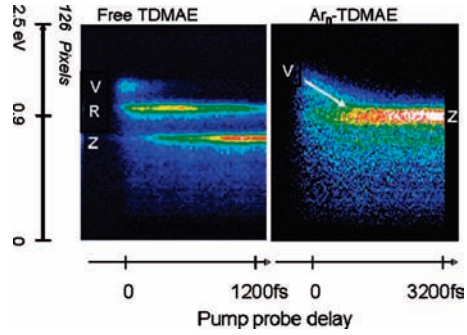

Figure 9. Comparison of anisotropic P_2 component in photoelectron spectra of free TDMAE (left) and deposited TDMAE (right). The evolution of the free molecule is well-accounted for by a sequential scheme V−R−Z.[20] The evolution of the spectrum of the deposited molecule in R is emphasized by a white arrow.

For deposited TDMAE, the electron images taken with a parallel pump and probe show smaller intensities for the P_2 component, but the presence of an anisotropic factor in the photoelectron spectra is unambiguous as in Figure 8. It corresponds to a β value of 0.35 for the Z state. This polarization is much less than for free TDMAE, where β is close to 0.8 for the same band. The most distinctive effect is the suppression of the low energy continuum in the anisotropic component P_2 of the spectra, as can be seen in Figure 7, by comparing the P_0 and P_2 components. The peak at 0.9 eV still contains a small low energy tail.

We therefore used the anisotropic component P_2 as the source of photoelectron time evolution in the following discussion, but we must bear in mind that it is a slightly biased source since the different energy components that we are about to describe in the photoelectron spectrum have different anisotropy factors (β). This is not important provided that we are not interested in the absolute value of each of the components but in their observation.

Time Decay Profiles in Photoelectron Spectra. We now turn to the description of the time-resolved photoelectron spectra of TDMAE deposited on Ar$_n$. In Figure 9, we compare the time-dependent spectra of the anisotropic components of free and deposited TDMAE spectra. In the free molecule, three bands are clearly visible on the left-hand side (Figure 9), displaying unambiguously a sequential decay. The highest energy band corresponding to V transforms into R and R into the lowest energy state Z.[20] At first sight, it is difficult to distinguish the same evolution on the cluster deposited spectra, where only two features are prominent in Figure 9, right: a high energy band extends to 2 eV (V) and grows within the autocorrelation time, as seen in Figure 6b, and a band at 0.9 eV rises in time (Z). A very weak feature is seen at 0.68 eV, identical to the Z band of the free molecule; this corresponds to the slight background of free TDMAE, as mentioned previously.

The data were analyzed iteratively. At first, we used the same three state sequential model as in ref 20 since in Figure 9, one can see that the two regions V and Z are connected together, allowing for the existence of another unseen band. In this way, we could simulate most of the cuts of the evolution at fixed energies and derive a decay time of 250 fs for V and a rise time for Z. However, the time evolution of Figure 10c could not be reproduced with the presence of a maximum at ∼600 fs. This is related to the evolution depicted by the arrow in Figure 9, which will be discussed later and assigned to the solvation of R over ∼0.5 eV. Solvation manifests itself in absorption spectra by a shift of the bands and a narrowing as it proceeds in a given electronic state. As time and frequency are thus related by what appears to be an approximate linear relationship in Figure 9 (right, arrow), a sliding Gaussian window was added to the sequential time evolution in R for the free molecule, $S_0(t)$,[20] leading to $S(t)$ for deposited TDMAE:

$$S(t) = S_0(t) \cdot \exp\left(-\left(\frac{t - 900^*(\Delta E/E)}{1600 - 0.2^*t}\right)^2\right) \quad (3)$$

The value of 900 fs represents a time constant for solvating the maximum available energy E between the initially populated state and the relaxed state, typically 0.6 eV. Thus, the window changes in position as the electron energy channel is fixed at ΔE and in width as time goes by with the 1600 fs constant.

The results are now reproduced in Figure 10, and again, band V can be identified on the cluster at the highest energies: a decay of 250 fs can be assigned to this component, as measured at 1.9 eV and reproduced in Figure 10a. The relevant photoelectron spectrum of species V is deduced from the spectrum recorded at the pump/probe autocorrelation, as appears in Figure 6b. This band, V, overlaps bands R and Z, the only one really distinct. Band Z is broader here for deposited TDMAE, while band R, well-separated in the free molecule, is apparent only indirectly. At 0.9 eV, band Z is observed to grow with a 1200 fs time constant as represented in Figure 10d. The rapid decay of V (250 fs) and the slow rise of Z (1200 fs) implies kinetically the existence of an intermediate R. This intermediate can be observed superimposed to V in the energy region of 1.8−1.3 eV and is shown in the fits of Figure 10 as the blue curve in the components. We can see from Figures 6a and 10a,b that between 1 and 2 eV, the time decay profile is continuously changing: a short decay with a 250 fs time constant, lengthening up to 1200 fs. In the fits of Figure 10, it appears clearly that the maximum of relaxed R as deduced from the kinetic analysis is located around 1.3−1.4 eV.

When comparing the photoelectron spectra of free and deposited TDMAE, the latter are more difficult to characterize because of a shift of the whole spectrum to higher energies and in a smaller energy range. The domain is 1−2 eV for bands V and Z in the deposited spectrum, as seen in Figure 9, while that of the free system is 0.68−1.8 eV. In addition, the van der Waals modes of the cluster broaden the spectrum notably. However, in both spectra at low electron energies, a similar broad background was simulated in velocity space by a Gaussian component (centered at pixel 40, 0.28 eV) as in Figure 6b. This background appears only in the isotropic photoelectron spectrum. The time evolution of this spectral component is similar to a step function convoluted by the autocorrelation. A slow rise component is only perceptible and can be accounted for by the P_2 component.

Lastly, the evolution of the spectrum of deposited TDMAE at long times was recorded as already mentioned with a 800 nm probe. This reveals an interesting difference with the free molecule. In Figure 11, both deposited TDMAE and free TDMAE (background) were recorded. It appears that the spectrum of the deposited molecule continues to evolve with a 10 ps time constant, while the free molecule has ceased to change.

Discussion

The combination of measurements in two different solvating environments—argon matrix and argon cluster, brings a rather precise description of the solvation effects on high excited states of molecules in organized media formed by argon atoms. Time-resolved experiments yielded the direct observation of stepwise

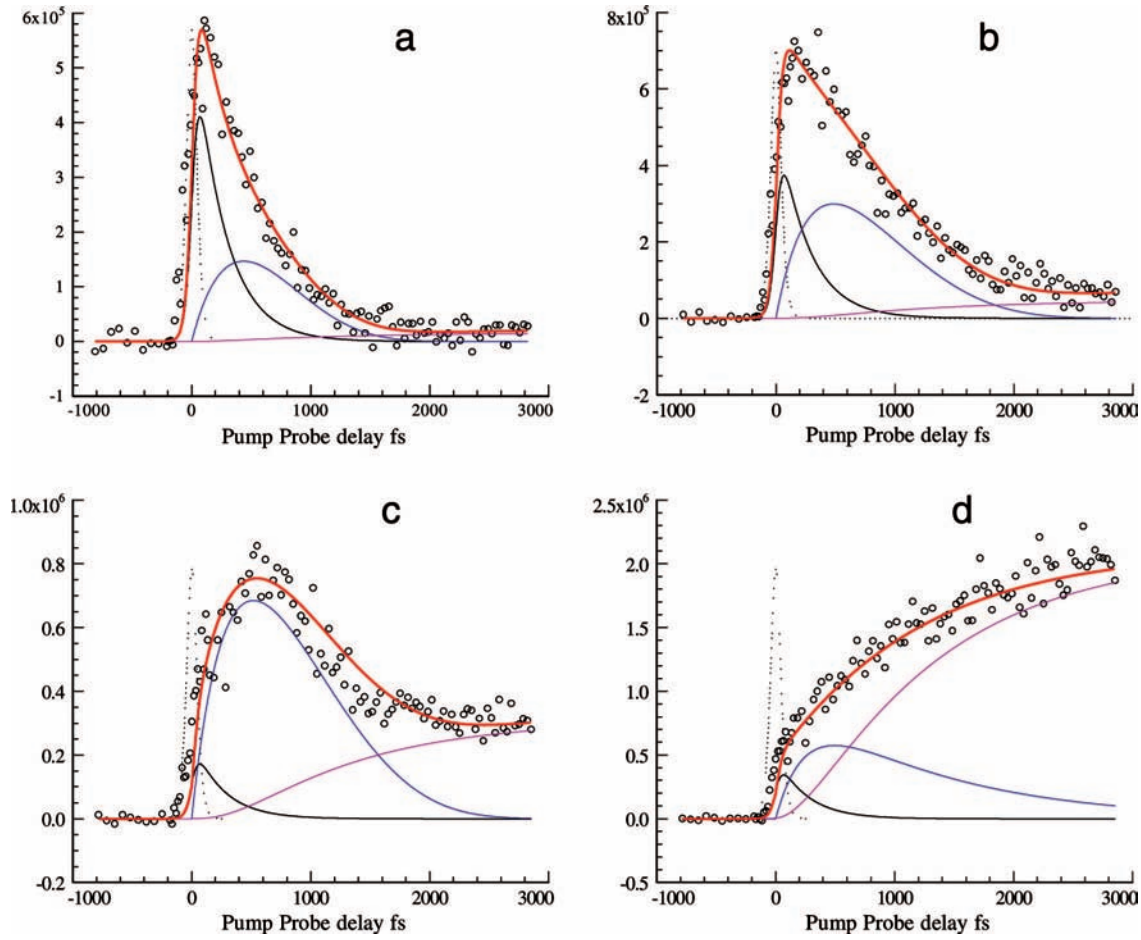

Figure 10. Time evolution of selected photoelectron energy regions of the P_2 component (angle averaged): (a) 1.9 eV, (b) 1.4 eV, (c) 1.3 eV, and (d) 0.9 eV.

solvation via photoelectron spectroscopy, while matrix isolation spectroscopy informed on the initial electronic level characters. The present discussion aims at giving a global picture of the mechanisms that are at play when TDMAE deposited on argon clusters was electronically excited.

The discussion is organized as follows. After reviewing the type of electronic levels in the free molecule, the actual effect of the solvent on the energy of these levels will be examined. Then, we discuss the nature of the intense band at 265 nm. The localization of the molecule on the clusters will be discussed in view of its ionization and autoionization processes in contact of the argon medium. The time-dependent dynamics as revealed by the photoelectron shifts will then be reviewed.

Energy Levels of Free Molecule and Its Solvation by Argon. The electronic structure of TDMAE is little known, aside from the fact that it retains some essential characteristics of ethylene, connected with a central double bond. There are very few calculations establishing the electronic structure and geometry of the molecule.[16,35–37] Basically, the C═C backbone of the molecule does not depart too far from planarity in the ground state and an electronic state with $\pi\pi^*$ character can be reached at 266 nm in the gas phase. This transition overlaps others belonging to states of Rydberg character, one of which starts below 400 nm, possibly 3s ← N. Therefore, the cluster or the matrix should differentially stabilize the states: the valence $\pi\pi^*$ to a minor extent, the Rydberg could be upshifted, while the ion $TDMAE^+$ will be stabilized by a charge induced dipole interaction.

Energy of Deposited TDMAE Ion. In a previous paper, where TDMAE was solvated within the interior of a cluster of ~60 argon atoms with two solvation shells, we estimated this interaction as leading to an ionization threshold no lower than 4.8 eV,[38] as compared to 5.4 eV in the gas phase.[16] If the molecule is at the surface of the argon cluster, the solvation shell is at least reduced by a factor of 2 (see Figure 2a), corresponding to a reduced number of interacting atoms. This leads to an ionization potential no lower than ~5.1 eV. This is confirmed by the ionization at short delay times with 266/800 nm. The energy of the outermost electron band generated by one 800 nm probe photon, from the deposited molecule, is at 0.44 eV shifted by 0.36 eV from the value of the free molecule. The argon environment diminishes thus the IP of the cluster down to ≈5.1 eV.

Energy Levels of Charge Transfer States in TDMAE. In the same way, all states containing charges should be stabilized by solvation. Thus, band Z, assigned to a transition to a zwitterionic state with a very strong dipole, should be stabilized by dipole−induced dipole interactions. Its stabilization should be smaller as compared to the ion, as the charges are less localized. In a similar fashion, the stabilization of the ion pair states of I_2 (I^+I^-) is much less than that of the ion in rare gas matrices.[28] This is explained by the fact that the more bulky I^- is destabilized and counteracts the stabilization of the positive smaller moiety. If we take an average ionization threshold for the clusters, its value should be 5.04 eV, from the preceding discussion, corresponding to a 0.36 eV shift in the IP of the cluster. This takes into account the distribution of solvation sites, owing to that of cluster sizes. If the stabilization of the ion and of Z are the same, the electron energy would not change for Z. Since the electron energy from the solvated Z state increases

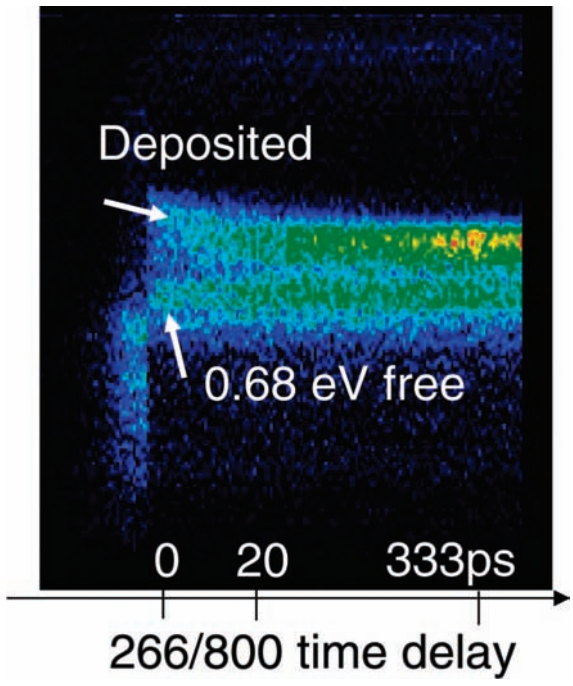

Figure 11. Time evolution of deposited TDMAE at long times of 0−333 ps observed by a two photon probe at 800 nm. The image is the time-dependent portion of the P_2 component of the photoelectron angular dependence, represented on a nonconstant double time scale of 0−20 and 20−330 ps. In this image, the free background molecule is also present at 0.68 eV. The upper component (deposited) varies in energy with time with a 10 ps time constant, while the lower component (free) is constant with time.

by 0.22 eV as compared to the free molecule, the latter Z state is only stabilized by 0.36–0.22 = 0.14 eV.

Energy of Rydberg Levels of Deposited TDMAE. On the contrary, Rydberg transitions are broadened, and the states of lower n are strongly upshifted in rare gas matrices.[29,39] The blue shift originates from a greater repulsion by the neighboring atoms in the matrix of Rydberg orbitals with sizes comparable to the cage radius. An example is given by NO in the argon matrix: the Rydberg bands are shifted by ∼0.8 eV and 10−40-fold broadened as compared to valence transitions. [27] This situation is different in clusters since the Rydberg atom or molecule on the cluster is relatively free. Indeed, for a small cluster, Hg−Ar in the 7s Rydberg state, a double well was found, a very shallow well at long distances (5.85 Å) relating to the van der Waals attraction and a deep one (at 2.8 Å) corresponding to a Hg^+−Ar core surrounded by an electron.[40,41] In this latter case, the argon atom is contained within the Rydberg orbital. This behavior also was characterized for small sodium−argon clusters ($n < 9$), where the 5s orbital surrounds an ionic cluster.[42] This shows that, depending on the initial configuration, the excitation of a Rydberg state may lead to different situations in the presence of perturbing (e.g., argon) atoms. Also, at the surface of the argon cluster, the symmetry of the Rydberg orbital is broken, and Rydberg states within a $nl\lambda$ complex can mix, yielding some configurations that are stabilized by the presence of the surface. A well-known example is the case of NO−Ar,[43] where 3pσ and 3pπ undergo strong mixing and form a new state. A similar situation may arise at the surface of an argon cluster; the Rydberg orbitals of the same n should mix (hybridize) to minimize the repulsion of the argon atoms. In addition, the repulsive energy contributions are likely to be compensated for by the strong interaction between the ionic core of the molecule and the surrounding Ar atoms as for matrix isolated NO in states $n \geq 5$.[44] Therefore, Rydberg states of deposited TDMAE could be stabilized with respect to the free molecule.

In the time-resolved photoelectron spectra of deposited TDMAE, the shift of the Rydberg intermediate state cannot be assigned with precision due to the overlap of the V, R, and Z bands that are much broader in the deposited cluster as compared to the free molecule as appears in Figure 9. These experimental facts contribute to the difficulty in distinguishing the signature of the R contribution in the photoelectron spectra of deposited TDMAE. The kinetic analysis allows us to assign the maximum of the Rydberg absorption at ∼1.2 eV or lower. We estimated in a first approximation that the level was stabilized in a range of 0−0.2 eV. However, as we simulated, the shape of the Rydberg transition strongly changes with time. If we simply look at Figure 9, for the free molecule, the intensities of R and Z are equivalent, which is no longer the case for the deposited molecule. Hence, the spectrum of R deposited at initial times is strongly broadened and evolves to a narrower form, taken into account in eq 3. This reduces the apparent intensity of Rydberg transitions of deposited TDMAE.

Nature of 266 nm Excitation. On the basis of the previous assignment of the matrix isolated spectra (Figures 4 and 5), the 266 nm band is assigned to a valence transition (N−V), based on the lack of a blue shift in the different matrices allowing for the comparison of excitation of the system at 266 nm in the different media: gas phase, cluster, and matrix. However, neon matrix spectra revealed two components to this band, the blue component having a Rydberg character. This component is likely shifted in the gas phase to lower energies. Nevertheless, this component will be the absorption at 266 nm since the observed decays in the isolated molecule show, in Figure 9a, a unique two step sequential evolution. This confirms that the excitation reaches a unique valence state; otherwise, we would have observed the simultaneous decay of two different states. The deviation to this scheme in the gas phase amounts to only a small background (∼5%) on the decay of V, which could be assigned to an underlying direct Rydberg excitation.

Anisotropy in Electron Distribution. The observation of anisotropic angular distributions of the electrons from clusters was quite a surprise since we expected the TDMAE molecule to be somehow buried in the cluster with $n = \sim 100$ argon atoms, after the thermalization following the pick-up process. There, the room temperature molecule captured by the argon cluster was cooled to 35 K while the excess energy is dissipated by the evaporation of surrounding argon atoms in the impact region. The atoms do not seem to reorganize around the TDMAE molecule, to embed it, since the polarization of the electron distributions can be explained only if, as represented in Figure 2a, some free space exists around the molecule. In the free solid angle, this allows for the ejection of electrons in a direction related to the polarization of the probe laser. There is simply no recollision of some of the electrons with the surrounding argon atoms (collision cross-section ∼2 $Å^2$; ref 45). On the other hand, as previously discussed, the energy of these electrons depends on the interaction of the molecule with the medium, taking into account the stabilization of the neutral and ionic TDMAE molecules. Thus, the degree of polarization as compared to that of the free molecule should be a measure of the free solid angle around TDMAE. The β value is actually ∼0.35 for the Z band, while it is close to 0.8 for the same band in the free molecule. Thus, we can infer that there is ≈1/2 of the space around the molecule, free for electron ejection. This is in agreement with the representation of the deposited cluster that

we have given in Figure 2, where TDMAE sits flat on the cluster in a quasi-substitutional site. One could imagine a more refined picture where the electrons emitted close to the argon surface would be gradually depolarized. This simple geometrical picture is also in agreement with the energy of the deposited ion cluster intermediate between the free molecule and the interior cluster.

Autoionization in Free TDMAE Molecule and Clusters. In the free molecule, it was shown that an isotropic component contributes to the photoelectron spectrum, the Gaussian component in Figure 8. The corresponding spectral distribution is displayed in the inset of Figure 7 and corresponds to a continuously decreasing function starting from $E = 0$. The two aspects of this photoelectron component, a monotonous decrease in intensity with energy, from $E = 0$, and the absence of polarization, points to autoionization as the underlying phenomenon competing with direct structured ionization. In the autoionization process, the Rydberg state accessed by the probe was core excited vibrationally or electronically. This excited state is vibronically coupled with the ground state ion, which causes the slow autoionization. The energy of the ion is distributed over many vibrational final states close to the neutral excited state; thus, the electron energy is close to zero. Also, the polarization of the electron is lost with respect to the initial state. Thus, we assign the unpolarized broad electron emission to electronic autoionization in accordance with earlier discussions.[46] There, we found that the lowest energy configuration of the TDMAE cation corresponded to a delocalized hole on the nitrogens, while vertical excitation from the π^* state leading to a π hole was energetically unfavorable; this implied an important contribution of autoionization to the ionization process.

The same broad continuum centered at zero energy in the isotropic component was found for the photoelectron deposited TDMAE. The additional Gaussian component had the same shape and relative intensity with respect to the isotropic spectrum, as appears in Figure 7. The fact that the autoionization contribution is globally the same as for the free molecule indicates a fast autoionization process, little affected by the medium. This shows that the intermolecular modes TDMAE−Ar do not contribute to the autoionization process here. However, when the ion or high Rydberg states are solvated in a very different way, the coupling scheme is modified. This will be the case when the ions are much more solvated than the Rydberg states, resulting in a higher gap and a faster and more efficient autoionization.[47] The small difference in the autoionization efficiency that we observed between the free and the deposited molecule is an indication that the energy of the highly autoionizing Rydberg states is stabilized in a similar way to the ion in the cluster.

Dynamics of Deposited TDMAE. There are two important aspects in the time evolution of the deposited molecule: the time scale of evolution and the behavior of each of the states. The time evolution of the deposited cluster excited at 266 nm was analyzed in a modified sequential three level scheme as compared to the free molecule. Two of the states, the initial valence V and terminal Z (in our time range of 0 −10 ps) straightforwardly were observed and assigned by comparison to the free molecule. The second state of Rydberg nature is more difficult to capture because its photoelectron spectrum overlaps both other spectra and notably the broad valence of lesser intensity in this photoelectron energy region (V is mostly observed in the isotropic P_0 spectrum).

Kinetically, the decay of V and the rise of Z with different time constants implies the existence of the R intermediate to which we assigned a 1200 fs time constant for the relaxed intermediate, from Figure 10d. The dynamics of this intermediate on the argon cluster is thus responsible for the lengthening by a factor of 3.5 as compared to the free molecule. Having assigned the intermediate to the same Rydberg state (or states) as in the free molecule, we recall the nature of this state. If in the free molecule several Rydberg states might be distinguished by their orbital symmetries, the presence of the argon cluster mixes them by loss of symmetry. If the valence state seems little affected by the cluster, the Rydberg state mediating the V−Z evolution should, as we already discussed, strongly be affected by the medium.

Indeed, when looking at the image in Figure 9(right), the photoelectron spectrum at early times and higher energies evolves continuously until Z is reached, as emphasized by the arrow. A kind of maximum evolves with time as shown by the arrow toward lower electron energies, in stark contrast to the behavior of the free molecule where three definite energies could be found. This also shows up by the existence of a maximum in the time evolution at ∼600 fs in Figure 10c. This behavior was simulated with the use of a sliding window implemented by eq 3. We exclude the possibility that TDMAE might be ejected from the surface of the cluster as excited metals can be[48] since (a) the kinetics is different from the bare molecule and (b) the Z band attained after relaxation of R is located at 0.9 eV instead of 0.68 eV in free TDMAE.

The gradual change in energy of R could correspond to the gradual relaxation of this Rydberg state within its environment. This relaxation can proceed (a) to a more stable electronic configuration with respect to the environment or (b) to Rydberg states of lower n values. On the other hand, the time scale, 600 fs, seems too short to be assigned to some progressive reorganization of the argon environment of the TDMAE molecule, which we shall see the evidence of later. We favor as the interpretation of this evolution the equilibration of the Rydberg molecule (process a), which is also witnessed in the slow down of the whole relaxation process in the cluster environment. The R−Z decay changes from 380 fs in the free molecule to 1200 fs in the deposited cluster. The major cause of this slow down is the loss of excess energy of the excited TDMAE molecule with respect to the Z state. Also, another cause might contribute to slow the relaxation of R in deposited TDMAE as compared to the free molecule: the inertial effect of the surrounding and interacting argon atoms, decreasing the frequencies of the moving groups.[38] Energy flowing to the argon atoms from the vibrational motion of TDMAE accompanies the relaxation, reducing the excess energy in TDMAE (R) and slowing down the evolution. This means that the adaptation process could correspond to a continuous solvation of the Rydberg state via the ion core of TDMAE that is left free by the mixed Rydberg orbital. This latter orbital will occupy the free space outside the cluster, allowing for interaction on the other side with TDMAE. This behavior is in striking contrast to the response of the medium in the case of a Rydberg excitation (NO 3sσ) in an argon matrix.[49] There, the medium has an instantaneous repulsive response to the creation of a bubble. On the contrary here, the TDMAE ion core is attracted by the cluster atoms. We also implicitly surmised in the preceding discussion that the R−V coupling initiating the evolution was unaffected by the argon atoms as the V−R decay seems unchanged by the presence of argon atoms (i.e., with a 250 fs time constant). The movement is direct from V to R for the wavepacket to traverse the conical intersection between the two surfaces and is only limited by the local slope of the

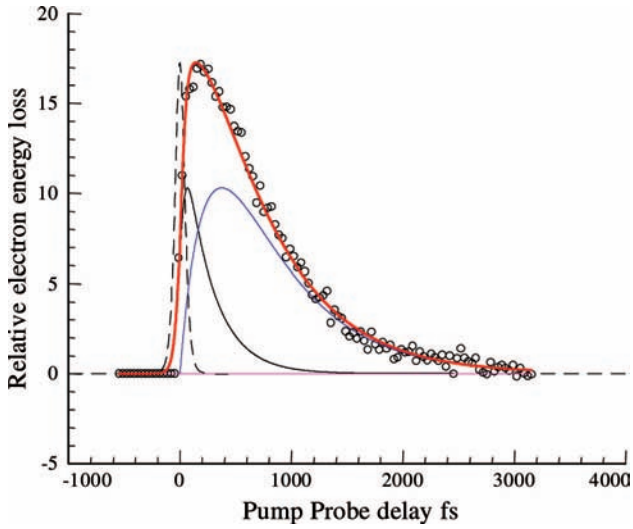

Figure 12. Time-dependent relative energy loss of the electron energy of the outer edge of the P_0 component of the photoelectron spectrum (see text). Red curve fit with a biexponential sequential evolution of 250 fs (black) + 600 fs (blue), convoluted with a 90 fs Gaussian pulse (dotted line).

potential, and this region does not seem strongly affected by the presence of argon atoms.

To characterize the solvation of the Rydberg band, we measured also the relative evolution of the photoelectron spectrum. This band is thoroughly overlapped with V and Z, but its high energy edge can serve as a reference of the relaxation. The correlation of the edge energies $E(t) - E(0)/(E(0) - E(\infty))$ characterizes the relaxation rate as displayed in Figure 12 and shows a lifetime of ~600 fs for this evolution. The simulation of this evolution is in accordance with the preceding kinetics showing a time lag of 250 fs for the initiation of the evolution. This lag corresponds to the lifetime of the V state, which is unaffected by the cluster before this relaxation operates. Thus, the evolution at early times of deposited TDMAE at the surface of argon can be described as the V−Z relaxation mediated by the gradual equilibration of a Rydberg intermediate with respect to the cluster.

It is important to mention that we observed wavepacket oscillations maintained for as long as 2.5 ps on the deposited cluster. These oscillations still appeared after electronic relaxation on the rise of the Z state, monitored via the isotropic term that has a higher intensity. This is a proof that coherence was maintained through the electronic relaxation of TDMAE on the cluster where the motion of the molecule is changed by the environment but not randomized. Despite the presence of the cluster, electronic relaxation still occurs via a wavepacket motion mechanism.

There is evidence that geometrical reorganization of the cluster occurs after the electronic relaxation to Z since the energy of the electrons originating from the Z state continues to decrease slowly in time with a 10 ps time constant. This time scale corresponds probably to several combined effects: cooling via evaporation of argon atoms and embedding the polarized system deeper in the cluster, while it is still plastic.

Conclusion

The stepwise solvation of the ethylenic TDMAE molecule by the presence of argon atoms was observed in a unique way by a combination of two methods: matrix isolation spectroscopy and photoelectron spectroscopy. Matrix isolation, by providing a static environment (a cage), allows the characterization of the nature of high electronic states, whereas time-resolved photoelectron spectroscopy shows the progressive solvation of the excited system at the surface of a cluster.

This revealed two effects of the medium on the electronic relaxation of a molecule involving polar and Rydberg states in the presence of argon clusters: one mostly electronic involving relaxation within the Rydberg manifold and the second corresponding to the stabilization with time of a polarized system at the surface of a cluster. This surface is a model system since it provides a way to evidence the specific influence of the solvation on each of the states involved in the cascade of the relaxation. The general trends of the mechanism operating in the free molecule are still effective here: relaxation from an initial valence state to a zwitterionic state through a Rydberg state. However, the medium has a dramatic effect in differentially lengthening the evolution on levels that it perturbs: the Rydberg states. We visualized the time-resolved stepwise solvation of these Rydberg states formed during the temporal evolution and observed their equilibration at the argon surface. This relaxation was interpreted here as the transition between different mixed Rydberg states existing only in the presence of the argon surface at times shorter than a few picoseconds. After 10 ps, the effect of the rearrangement on the argon atoms could be observed. Here, the Rydberg states were accessed in the process of electronic relaxation and not directly as absorption did not allow. Recently, we applied with success this methodology to directly access Rydberg states of a large molecule, DABCO, showing similar relaxation steps starting from the Rydberg manifold.

Acknowledgment. The authors thank the technical team at LUCA for developing, maintaining, and running the femtosecond laser facility (Laser Ultra-Court Accordable) of the CEA, DSM/IRAMIS. This work was supported by the Swiss−French collaboration contract PAI "Germaine de Staël" JH/RE82/221590.

References and Notes

(1) Jortner, J.; Rice, S. A.; Hochstrasser, R. M. *Advances in Photochemistry*; Pitts, J. N., Jr., Hammond, G. S., Noyes, W. Albert, Jr.; Interscience Publishers (a division of John Wiley & Sons): New York, 1969; Vol. 7, p 149.
(2) Teller, E. *J. Phys. Chem.* **1937**, *41*, 109–116.
(3) Lahmani, F.; Tramer, A.; Tric, C. *J. Chem. Phys.* **1974**, *60*, 4431–4447.
(4) Grimbert, D.; Lavollee, M.; Nitzan, A.; Tramer, A. *Chem. Phys. Lett.* **1978**, *57* (1), 45–49.
(5) Viel, A.; Krawczyk, R. P.; Manthe, U.; Domcke, W. *J. Chem. Phys.* **2004**, *120* (23), 11000–11010.
(6) Quenneville, J.; Ben-Nun, M.; Martinez, T. J. *J. Photochem. Photobiol., A* **2001**, *144* (2−3), 229–235.
(7) Ben Nun, M.; Martinez, T. J. *Chem. Phys.* **2000**, *259*, 237–248.
(8) Ben-Nun, M.; Martinez, T. J. *Chem. Phys. Lett.* **1998**, *298* (1−3), 57–65.
(9) Barbatti, M.; Paier, J.; Lischka, H. *J. Chem. Phys.* **2004**, *121* (23), 11614–11624.
(10) Farmanara, P.; Stert, V.; Radloff, W. *Chem. Phys. Lett.* **1998**, *288*, 518–522.
(11) Mestdagh, J. M.; Visticot, J. P.; Elhanine, M.; Soep, B. *J. Chem. Phys.* **2000**, *113*, 237–248.
(12) Blanchet, V.; Zgierski, M.; Seideman, T.; Stolow, A. *Nature (London, U.K.)* **1999**, *401*, 52–54.
(13) Pedersen, S.; Banares, L.; Zewail, A. H. *J. Chem. Phys.* **1992**, *97* (11), 8801–8804.
(14) Fuss, W.; Lochbrunner, S.; Muller, A. M.; Schikarski, T.; Schmid, W. E.; Trushin, S. A. *Chem. Phys.* **1998**, *232* (1-2), 161−174.
(15) Cyr, D. R.; Hayden, C. C. *J. Chem. Phys.* **1996**, *104*, 771–774.
(16) Nakato, Y.; Ozaki, M.; Tsubomura, H. *Bull. Chem. Soc. Jpn.* **1972**, *45*, 1299–1305.
(17) Salem, L. *Science (Washington, DC, U.S.)* **1976**, *191*, 822–830.
(18) Salem, L. *Electrons in Chemical Reactions: First Principles*; John Wiley & Sons: New York, 1982.

(19) Muller, T.; Dallos, M.; Lischka, H. *J. Chem. Phys.* **1999**, *110* (15), 7176–7184.

(20) Gloaguen, E.; Mestdagh, J. M.; Poisson, L.; Lepetit, F.; Visticot, J. P.; Soep, B.; Coroiu, M.; Eppink, A. T. J. B.; Parker, D. H. *J. Am. Chem. Soc.* **2005**, *127* (47), 16529–16534.

(21) Syage, J. A. *Zeitschrift fur Physik D—Atoms, Molecules, and Clusters* **1994**, *30*, 1–12.

(22) Loginov, E.; Rossi, D.; Drabbels, M. *Phys. Rev. Lett.* **2005**, *95* (16), 163401–163414.

(23) Bragg, A. E.; Verlet, J. R. R.; Kammrath, A.; Cheshnovsky, O.; Neumark, D. M. *Science (Washington, DC, U.S.)* **2004**, *306* (5696), 669–671.

(24) Neumark, D. M. *J. Chem. Phys.* **2006**, *125* (13), 132303–132315.

(25) Winter, B.; Weber, R.; Hertel, I. V.; Faubel, M.; Vrbka, L.; Jungwirth, P. *Chem. Phys. Lett.* **2005**, *410* (4−6), 222–227.

(26) Verlet, J. R. R.; Bragg, A. E.; Kammrath, A.; Cheshnovsky, O.; Neumark, D. M. *Science (Washington, DC, U.S.)* **2005**, *307* (5706), 93–96.

(27) Chergui, M.; Schwentner, N.; Chandrasekharan, V. *Phys. Rev. Lett.* **1991**, *66* (19), 2499–2502.

(28) Helbing, J.; Chergui, M. *J. Chem. Phys.* **2001**, *115* (13), 6158–6172.

(29) Chergui, M.; Schwentner, N.; Bohmer, W. *J. Chem. Phys.* **1986**, *85* (5), 2472–2482.

(30) Hagena, O. F. *Z. Phys. D: At., Mol. Clusters* **1987**, *4* (3), 291–299.

(31) Buck, U.; Krohne, R. *J. Chem. Phys.* **1996**, *105* (13), 5408–5415.

(32) Garcia, G. A.; Nahon, L.; Powis, I. *Rev. Sci. Instrum.* **2004**, *75* (11), 4989–4996.

(33) Robin, M. B. *Higher Excited States of Polyatomic Molecules*; Academic Press: San Diego, 1975; Vol. 2, pp 199−202.

(34) Velarde, L.; Habteyes, T.; Grumbling, E. R.; Pichugin, K.; Sanov, A. *J. Chem. Phys.* **2007**, *127*, 084302-6.

(35) Tanaka, K.; Sato, T.; Yamabe, T. *J. Phys. Chem.* **1996**, *100*, 3980–3982.

(36) Pokhodnia, K. I.; Papavassiliou, J.; Umek, P.; Omerzu, A.; Mihailovic, D. *J. Chem. Phys.* **1999**, *110* (7), 3606–3611.

(37) Fleurat-Lessard, P.; Volatron, F. *J. Phys. Chem. A* **1998**, *102*, 10151–10158.

(38) Sorgues, S.; Mestdagh, J.-M.; Soep, B.; Visticot, J.-P. *Chem. Phys.* **2004**, *301*, 225–237.

(39) Gedanken, A.; Raz, B.; Jortner, J. *J. Chem. Phys.* **1973**, *58* (3), 1178–1194.

(40) Duval, M. C.; D'Azy, O. B.; Breckenridge, W. H.; Jouvet, C.; Soep, B. *J. Chem. Phys.* **1986**, *85* (11), 6324–6334.

(41) Onda, K.; Yamanouchi, K. *J. Chem. Phys.* **1995**, *102* (3), 1129–1140.

(42) Rhouma, M. B. E. H.; Lakhdar, Z. B.; Berriche, H.; Spiegelman, F. *J. Chem. Phys.* **2006**, *125* (8), 84315−84311.

(43) Shafizadeh, N.; Brechignac, P.; Dyndgaard, M.; Fillion, J. H.; Gauyacq, D.; Levy, B.; Miller, J. C.; Pino, T.; Raoult, M. *J. Chem. Phys.* **1998**, *108* (22), 9313–9326.

(44) Vigliotti, F.; Chergui, M. *Eur. Phys. J. D* **2000**, *10* (3), 379–390.

(45) Buckman, S. J.; Lohmann, B. *J. Phys. B: At., Mol., Opt. Phys.* **1986**, *19* (16), 2547–2564.

(46) Sorgues, S.; Mestdagh, J.-M.; Gloaguen, E.; Visticot, J.-P.; Heninger, M.; Mestdagh, H.; Soep, B. Investigation of ion−molecule reactions via femtosecond excitation and ionization of [tetrakis(dimethylamino)ethylene]$_{n\geq 1}$. *J. Phys. Chem. A* **2004**, 3884–3895.

(47) Reininger, R.; Saile, V.; Laporte, P. *Phys. Rev. Lett.* **1985**, *54* (11), 1146–1149.

(48) Visticot, J. P.; de Pujo, P.; Mestdagh, J. M.; Lallement, A.; Berlande, J.; Sublemontier, O.; Meynadier, P.; Cuvellier, J. *J. Chem. Phys.* **1994**, *100* (1), 158–164.

(49) Jeannin, C.; Portella-Oberli, M. T.; Jimenez, S.; Vigliotti, F.; Lang, B.; Chergui, M. *Chem. Phys. Lett.* **2000**, *316* (1−2), 51–59.

JP711259M